

## Interfaces Between two Dissimilar Elastic Materials

Chyanbin Hwu<sup>1</sup>, T.L. Kuo and Y.C. Chen

**Abstract:** In this paper the near tip solutions for interface corners written in terms of the stress intensity factors are presented in a unified expression. This single expression is applicable for any kinds of interface corners including corners and cracks in homogeneous materials as well as interface corners and interface cracks lying between two dissimilar materials, in which the materials can be any kinds of linear elastic anisotropic materials or piezoelectric materials. Through this unified expression of near tip solutions, the singular orders of stresses and their associated stress/electric intensity factors for different kinds of interface problems can be determined through the same formulae and solution techniques. This unified feature of solving interface problems is then implemented numerically through several different interface problems. Moreover, in order to improve the accuracy and efficiency of numerical computation, a special boundary element based upon the Green's function of bimetals is introduced in this paper.

**Keywords:** interface cracks, interface corners, singular orders of stresses, stress intensity factors, anisotropic materials, piezoelectric materials, finite element method, boundary element method

### 1 Introduction

Due to the mismatch of elastic properties, stress singularity usually occurs near the tips of interface corners/cracks between two dissimilar materials, which may initiate failure of materials and structures. The singular order of stresses near the interface corners/cracks is a good index for the understanding of failure initiation. However, in engineering applications one usually feels only the knowledge of singular orders is not enough for the prediction of failure initiation since it only reflects the local combination and is nothing to do with the far-field environment and the external loading condition. These global influential factors are reflected through another important parameter – stress intensity factor. Therefore, for interface prob-

---

<sup>1</sup> Institute of Aeronautics and Astronautics, National Cheng Kung University, Tainan, Taiwan, R.O.C. Tel: 886-6-2757575 ext.63662; Fax: 886-6-2389940; E-mail: CHwu@mail.ncku.edu.tw

lems it is important to know the singular orders as well as their associated stress intensity factors. However, due to the complexity of stresses near the tip of interface corners/cracks, most of the existing calculation methods will encounter the problem of accuracy and convergency. To solve this problem, several different approaches have been proposed in the literature, such as (Raju and Newmann, 1977; Li, *et al.*, 1998; Labossiere and Dunn, 1999; Sukumar, *et al.*, 2000; Ou *et al.*, 2003; Shah, *et al.*, 2006; Sanz *et al.*, 2007; Hwu and Ikeda, 2008; Attaporn and Koguchi, 2009). In this paper, two approaches introduced recently will be discussed. One is the improvement of the computational method for stress intensity factors by establishing a path independent H-integral for general interface problems (Hwu and Kuo, 2007), and the other is the improvement of boundary element method by including the fundamental solution of bimetals.

In addition to the improvement of computational method for interface problems, in this paper we like to emphasize the *unified* characteristics of the method introduced here for the interface corners/cracks. In other words, the formulae and solution techniques introduced in this paper are applicable for any kinds of anisotropic materials and piezoelectric materials, as well as any kinds of corners including cracks, interface cracks, corners and interface corners. Moreover, through the modification of H-integral, they are valid not only for two dimensional problems but also for three dimensional problems (Kuo and Hwu, 2009).

## 2 Near tip solutions for interface cracks and corners

By employing Stroh formalism for anisotropic elasticity, the near tip solution for interface cracks and corners can be written in terms of the stress intensity factors as (Hwu, *et al.*, 2003; Hwu and Kuo, 2007; Hwu and Ikeda, 2008)

$$\begin{aligned} \mathbf{u}(r, \theta) &= \frac{1}{\sqrt{2\pi}} r^{1-\delta_R} \mathbf{V}(\theta) \langle (1 - \delta_R + i\varepsilon_\alpha)^{-1} (r/\ell)^{i\varepsilon_\alpha} \rangle \mathbf{\Lambda}^{-1} \mathbf{k}, \\ \phi(r, \theta) &= \frac{1}{\sqrt{2\pi}} r^{1-\delta_R} \mathbf{\Lambda}(\theta) \langle (1 - \delta_R + i\varepsilon_\alpha)^{-1} (r/\ell)^{i\varepsilon_\alpha} \rangle \mathbf{\Lambda}^{-1} \mathbf{k}, \end{aligned} \quad (1)$$

in which  $\mathbf{u}$  and  $\phi$  are, respectively, the *displacement vector* and *stress function vector*;  $\mathbf{k}$  is a vector containing different modes of *stress intensity factors*;  $(r, \theta)$  is the polar coordinate with origin located on the tip of cracks/corners (Figure 1); the angular bracket  $\langle \rangle$  stands for a diagonal matrix in which each component is varied according to the subscript  $\alpha$ , and the range of the subscript is 1 to 3 for general anisotropic materials and is 1 to 4 for piezoelectric materials;  $\delta_R$  and  $\varepsilon_\alpha$  are, respectively, the real and imaginary part of the *most critical singular order*  $\delta_c$  which is located in the range of  $0 < \delta_R < 1$ , and sometimes  $\varepsilon_\alpha$  is also called *oscillatory index*;  $\ell$  is a length parameter which may be chosen arbitrarily as long

as it is held fixed when specimens of a given material pair are compared;  $\mathbf{V}(\theta)$  and  $\mathbf{\Lambda}(\theta)$  are *eigenfunction matrices* of displacement and stress function, and  $\mathbf{\Lambda} = \mathbf{\Lambda}(0)$  whose detailed expressions can be found in (Hwu and Kuo, 2007; Hwu and Ikeda, 2008).

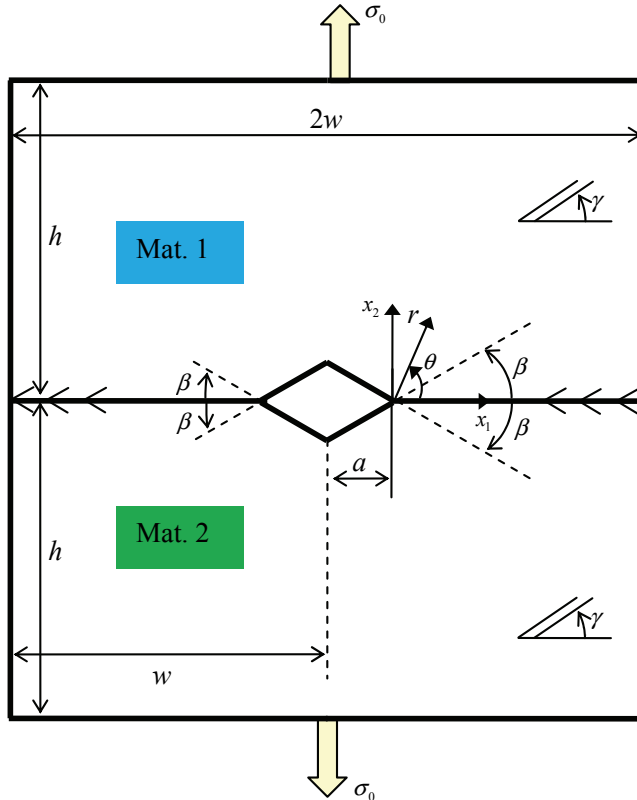


Figure 1: A center interface corner between two dissimilar materials.

The stresses are related to the stress functions by (Hwu and Ikeda, 2008)

$$\boldsymbol{\sigma} = \mathbf{\Omega}(\theta)\boldsymbol{\phi}_{,r}(r, \theta) = \frac{1}{\sqrt{2\pi}}r^{-\delta_R}\mathbf{\Omega}(\theta)\mathbf{\Lambda}(\theta) \langle (r/\ell)^{i\varepsilon\alpha} \rangle \mathbf{\Lambda}^{-1}\mathbf{k}, \quad (2)$$

where the subscript comma stands for differentiation, and  $\boldsymbol{\sigma}$  and  $\mathbf{\Omega}(\theta)$  denote, re-

spectively, the *stress vector* and *transformation matrix*, and

$$\boldsymbol{\sigma} = \begin{Bmatrix} \sigma_{r\theta} \\ \sigma_{\theta\theta} \\ \sigma_{\theta 3} \end{Bmatrix}, \mathbf{k} = \begin{Bmatrix} K_{II} \\ K_I \\ K_{III} \end{Bmatrix},$$

$$\boldsymbol{\Omega}(\theta) = \begin{bmatrix} \cos \theta & \sin \theta & 0 \\ -\sin \theta & \cos \theta & 0 \\ 0 & 0 & 1 \end{bmatrix}, \text{ for anisotropic materials,}$$

$$\boldsymbol{\sigma} = \begin{Bmatrix} \sigma_{r\theta} \\ \sigma_{\theta\theta} \\ \sigma_{\theta 3} \\ D_\theta \end{Bmatrix}, \mathbf{k} = \begin{Bmatrix} K_{II} \\ K_I \\ K_{III} \\ K_{IV} \end{Bmatrix}, \quad (3)$$

$$\boldsymbol{\Omega}(\theta) = \begin{bmatrix} \cos \theta & \sin \theta & 0 & 0 \\ -\sin \theta & \cos \theta & 0 & 0 \\ 0 & 0 & 1 & 0 \\ 0 & 0 & 0 & 1 \end{bmatrix}, \text{ for piezoelectric materials.}$$

In the above,  $(\sigma_{r\theta}, \sigma_{\theta\theta}, \sigma_{\theta 3})$  and  $D_\theta$  are the components of stresses and electric displacements in polar coordinate, and  $K_I, K_{II}, K_{III}$  and  $K_{IV}$  are the stress intensity factors of opening mode, shearing mode, tearing mode and electric mode.

### 3 Singular orders of stresses

The near tip solutions shown in eqn.(1) are the solutions associated with the singular order  $\delta = \delta_R + i\varepsilon_\alpha$ , in which the singular order should be determined through the satisfaction of boundary conditions for interface corners/cracks. By employing Stroh formalism for the general multi-bonded wedges, the orders of stress singularity can be determined by the following eigen-relation (Hwu, *et al.*, 2003; Hwu and Lee, 2004; Hwu and Ikeda, 2008), which is valid for cracks, interface cracks, corners and interface corners, and the materials can be any kinds of linear elastic anisotropic materials or piezoelectric materials.

bonded:  $\|\mathbf{K}_e - \mathbf{I}\| = 0$ ,

free - free:  $\|\mathbf{K}_e^{(3)}\| = 0$ , fixed - fixed:  $\|\mathbf{K}_e^{(2)}\| = 0$ , (4)

free - fixed:  $\|\mathbf{K}_e^{(1)}\| = 0$ , fixed - free:  $\|\mathbf{K}_e^{(4)}\| = 0$ ,

where  $\mathbf{K}_e^{(i)}, i = 1, 2, 3, 4$  are the submatrices of  $\mathbf{K}_e$  defined by

$$\mathbf{K}_e = \begin{bmatrix} \mathbf{K}_e^{(1)} & \mathbf{K}_e^{(2)} \\ \mathbf{K}_e^{(3)} & \mathbf{K}_e^{(4)} \end{bmatrix}, \mathbf{K}_e = \prod_{k=1}^n \mathbf{E}_{n-k+1} = \mathbf{E}_n \mathbf{E}_{n-1} \dots \mathbf{E}_1, \quad (5a)$$

and

$$\mathbf{E}_k = \hat{\mathbf{N}}_k^{1-\delta}(\theta_k, \theta_{k-1}), \quad k = 1, 2, 3, \dots, n. \quad (5b)$$

$\theta_k, \theta_{k-1}$  are the angular location of the two sides of the  $k$ th wedge, and  $\hat{\mathbf{N}}$  is the key matrix defined by

$$\hat{\mathbf{N}}(\theta, \alpha) = \cos(\theta - \alpha)\mathbf{I} + \sin(\theta - \alpha)\mathbf{N}(\alpha), \quad (6)$$

where  $\mathbf{I}$  is a unit matrix and  $\mathbf{N}(\alpha)$  is the *generalized fundamental elasticity matrix* of  $\mathbf{N}$  (Ting, 1996). The  $\delta$  appeared in the power of key matrix  $\hat{\mathbf{N}}$  in (5b) is the *singular order* to be determined, which may be positive or negative or zero, real or complex, repeated or distinct. If the stress singularity is concerned and the strain energy should be bounded, only the region  $0 < Re(\delta) < 1$  is considered. Note that the generalized fundamental elasticity matrix  $\mathbf{N}(\alpha)$  is a  $6 \times 6$  matrix for anisotropic materials and is a  $8 \times 8$  matrix for piezoelectric materials.

#### 4 Stress intensity factors

A unified definition of stress intensity factors which correspond to the most critical singular order  $\delta_c$  and are valid for cracks, interface cracks, corners and interface corners, and anisotropic and piezoelectric materials was proposed as (Hwu and Kuo, 2007; Hwu and Ikeda, 2008)

$$\mathbf{k} = \lim_{r \rightarrow 0} \sqrt{2\pi r}^{\delta_R} \mathbf{\Lambda} \langle (r/\ell)^{-i\varepsilon_\alpha} \rangle \mathbf{\Lambda}^{-1} \boldsymbol{\phi}_{,r}(r, 0). \quad (7)$$

To provide a stable and efficient computing approach for the general mixed-mode stress intensity factors, the path-independent H-integral based on reciprocal theorem of Betti and Rayleigh was established in (Hwu and Kuo, 2007) for 2D problems and in (Kuo and Hwu, 2009) for 3D problems, i.e.,

$$\begin{aligned} 2D: H &= \int_{\Gamma} (\mathbf{u}^T \hat{\mathbf{t}} - \hat{\mathbf{u}}^T \mathbf{t}) d\Gamma, \\ 3D: H &= \int_{\Gamma} (\mathbf{u}^T \hat{\mathbf{t}} - \hat{\mathbf{u}}^T \mathbf{t}) d\Gamma + \int_{S_{\Gamma}} (\hat{\sigma}_{i3,3} u_i + \hat{\sigma}_{i3} u_{i,3} - \sigma_{i3,3} \hat{u}_i - \sigma_{i3} \hat{u}_{i,3}) dS, \end{aligned} \quad (8)$$

in which  $\mathbf{u}$  and  $\mathbf{t}$  are the displacement and traction vectors of the actual system that can be obtained from any appropriate method such as finite element or boundary element or experimental testing, and  $\hat{\mathbf{u}}$  and  $\hat{\mathbf{t}}$  are those of the complementary system which is the near tip solution with singular order  $\delta$  replaced by  $2 - \delta$ ; the path  $\Gamma$  emanates from the lower corner flank and terminates on the upper corner flank

in counterclockwise direction. For piezoelectric materials, the fourth component of traction vector  $\mathbf{t}$  is surface electric displacement and the fourth component of displacement vector  $\mathbf{u}$  is the electric potential.

By using the near tip solutions obtained in the literature (Hwu and Kuo, 2007), it has been proved that the stress intensity factor  $\mathbf{k}$  is related to the path-independent H-integral by

$$\mathbf{k} = \sqrt{2\pi\Lambda} \langle (1 - \delta_R + i\varepsilon_\alpha) \ell^{i\varepsilon_\alpha} \rangle \mathbf{H}^{*-1} \mathbf{h}, \quad (9)$$

where

$$\mathbf{H}^* = \int_{\theta_0}^{\theta_n} [\hat{\mathbf{\Lambda}}'^T(\theta) \mathbf{V}(\theta) - \hat{\mathbf{V}}^T(\theta) \mathbf{\Lambda}'(\theta)] d\theta, \quad (10)$$

and  $\mathbf{h}$  is a vector consisting the value of H-integral calculated with certain specified complementary solutions.

## 5 Corner types – cracks, corners, interface cracks or interface corners

To show that the above formulae are valid for several different kinds of cracks and corners, four examples are illustrated in this section. They are: a center crack in a homogeneous anisotropic material, a center corner in a homogeneous anisotropic material, an interface crack between two dissimilar anisotropic materials, an interface corner between two dissimilar anisotropic materials. Although some typical problems of interface cracks/corners have been presented in our previous paper (Hwu and Kuo, 2007), for the purpose of comparison most of the examples illustrated in that paper are calculated for isotropic materials. To show that the formulae and their associated solution techniques are valid for any kinds of anisotropic materials, here we like to extend the examples to the general anisotropic materials. Moreover, to study the connection between cracks, corners, interface cracks and interface corners, a particular problem is designed in Figure 1. From this Figure, we see that when  $\beta = 0$  the corner problems will be reduced to crack problems, and when material 1 and material 2 are chosen to be the same material the interface corners/cracks will be reduced to the corners/cracks in homogeneous materials. Without loss of generality, in all examples the calculation of singular orders and stress intensity factors is focused on the right tip of crack/corner.

### *Example 1: a center crack in a homogeneous anisotropic material*

A center crack with size  $2a$  in an infinite anisotropic plate subjected to remote tension  $\sigma$  is a classical problem in fracture mechanics, which is usually used as the first check for the advanced studies. It is well known that both of the singular order and stress intensity factor of this problem are independent of the material

properties, and are obtained analytically as  $\delta = 0.5$ ,  $K_I = \sigma\sqrt{\pi a}$  and  $K_{II} = K_{III} = 0$ . To check our results by this classical problem, in Figure 1 the crack is simulated by letting  $\beta = 0^0$ , the infinite plate is approximated by setting  $h = 30a$  and  $w = 31a$ , the homogeneous material is made by selecting two identical materials, and the anisotropic material is made by rotating the principal direction of an orthotropic material  $\gamma$  degree. The numerical data used for our testing is then given by  $a = 0.01\text{m}$ ,  $\sigma_0 = 1\text{MPa}$ ,  $\gamma = 30^0$  and

$$\begin{aligned} E_{11} &= 134.45\text{GPa}, E_{22} = E_{33} = 11.03\text{GPa}, \\ G_{12} &= G_{13} = 5.84\text{GPa}, G_{23} = 2.98\text{GPa}, \\ \nu_{12} &= \nu_{13} = 0.301, \nu_{23} = 0.49. \end{aligned}$$

With the above numerical data, the singular order calculated from (4) is obtained as  $\delta = 0.5$  which is a triple root, and the stress intensity factors calculated from H-integral, i.e., from (8)<sub>1</sub> and (9), are obtained as

$$K_I = 0.178\text{MPa}\sqrt{\text{m}}, K_{II} = 0.000107\text{MPa}\sqrt{\text{m}}, K_{III} = 0.$$

It can easily be seen that all these values agree very well with the analytical solutions provided in the literature.

*Example 2: a center corner in a homogeneous anisotropic material*

In this example, the center corner is represented by letting  $\beta = 30^0$  in Figure 1 and all the other geometrical and material properties are the same as Example 1. By using the same formulae and solution techniques as center cracks stated in Example 1, the singular orders and stress intensity factors of this problem are calculated as

$$\begin{aligned} \delta &= 0.478, \\ K_I &= 0.254\text{MPa} \times \text{m}^{0.478}, K_{II} = 0.104\text{MPa} \times \text{m}^{0.478}, K_{III} = 0. \end{aligned}$$

Through this result, we see that both of  $K_I$  and  $K_{II}$  increase due to the change from crack to corner when they are compared under different units.

*Example 3: an interface crack between two dissimilar materials*

In this example, material 2 has the same properties as the orthotropic material mentioned in example 1 with  $\gamma = 30^0$ , while material 1 is chosen to be an isotropic one which possess Young's modulus  $E = 10\text{GPa}$  and Poisson's ratio  $\nu = 0.2$ . All the other geometrical and material properties are the same as example 1. The reference length used in the definition (7) is selected to be half of the crack length, i.e.,  $\ell = 0.01\text{m}$ .

Again through the same solution techniques, the singular orders and stress intensity factors of this problem are calculated as

$$\delta = 0.5 \pm 0.063i,$$

$$K_I = 0.180\text{MPa}\sqrt{\text{m}}, K_{II} = 0.024\text{MPa}\sqrt{\text{m}}, K_{III} = 0.$$

which agree with the analytical solutions provided in (Hwu, 1993). Through the comparison with example 1, we see that both  $K_I$  and  $K_{II}$  increase due to the difference of mechanical properties between material 1 and material 2.

*Example 4: an interface corner between two dissimilar materials*

Same as example 3 except that  $\beta = 30^\circ$  for interface corner. The singular orders and stress intensity factors of this problem are calculated as

$$\delta = 0.473,$$

$$K_I = 0.227\text{MPa} \times \text{m}^{0.473}, K_{II} = -0.048\text{MPa} \times \text{m}^{0.473}, K_{III} = 0.$$

Again, like the crack/corner in homogeneous materials, by comparison with example 3, we see that both of  $K_I$  and  $K_{II}$  increase due to the change from crack to corner when they are compared under different units. However, unlike cracks in homogeneous materials or on the interface of bimetals compared in examples 1 and 3, through the comparison with example 2, we see that both the magnitudes of  $K_I$  and  $K_{II}$  decrease instead of increase due to the difference of mechanical properties between material 1 and material 2.

## 6 Material types – anisotropic or piezoelectric

To show that the formulae and solution techniques presented in this paper can also be extended to the piezoelectric materials, the interface crack/corner between two dissimilar piezoelectric materials will be discussed in this section through example 5. To see the piezo effects, examples 3 and 4 will be reconsidered by letting the anisotropic material be the one of piezoelectric materials excluding the piezoelectric constants.

*Example 5: an interface crack/corner between two dissimilar piezoelectric materials*

Examples 3 and 4 are reconsidered here by replacing the anisotropic materials with the piezoelectric materials PZT-7A and PZT-5H whose material properties are listed in Table 1. For both cases, PZT-7A and PZT-5H with  $\gamma = 0^\circ$  are employed to constitute material 1 and material 2 (see Figure 1), respectively. All the other geometrical dimensions are the same as examples 3 and 4. A uniform remote

tension  $\sigma_0 = 1\text{MPa}$  is applied on the two horizontal edges, while a uniform electric flux density  $D_0 = -0.001\text{C/m}^2$  and an electric constraint  $u_4 = 0$  are, respectively, specified on the bottom edge and top edge. The singular orders calculated from (4) and the stress/electric intensity factors calculated from H-integral, i.e., from (8)<sub>1</sub> and (9), are obtained as follows.

Table 1: Material constants of PZT-5H and PZT-7A.

	PZT-5H	PZT-7A
$C_{11}, C_{33}[\text{GPa}]$	126	148
$C_{12}, C_{23}[\text{GPa}]$	53	74.2
$C_{13}[\text{GPa}]$	55	76.2
$C_{22}[\text{GPa}]$	117	131
$C_{44}, C_{66}[\text{GPa}]$	35.3	25.4
$C_{55}[\text{GPa}]$	35.5	55.9
$e_{21}[\text{C/m}^2]$	-6.5	-2.1
$e_{22}[\text{C/m}^2]$	23.3	9.5
$e_{23}[\text{C/m}^2]$	-6.5	-2.1
$e_{16}, e_{34}[\text{C/m}^2]$	17	9.7
$\omega_{11}, \omega_{33}[10^{-9} \text{C}/(\text{V m})]$	15.1	8.11
$\omega_{22}[10^{-9} \text{C}/(\text{V m})]$	13	7.35

Interface crack:

$$\delta = 0.5 \pm 0.007i, 0.5, 0.5,$$

$$K_I = 0.177\text{MPa}\sqrt{\text{m}}, K_{II} = -0.016\text{MPa}\sqrt{\text{m}},$$

$$K_{III} = 0, K_{IV} = 0.177 \times 10^{-3}(\text{C/m}^2)\sqrt{\text{m}},$$

which agree very well with the analytical solutions provided in the literature (Hwu and Ikeda, 2008).

Interface corner:

$$\delta = 0.486,$$

$$K_I = 0.218\text{MPa} \times \text{m}^{0.486}, K_{II} = 0.025\text{MPa} \times \text{m}^{0.486},$$

$$K_{III} = 0, K_{IV} = 0.043 \times 10^{-3}(\text{C/m}^2) \times \text{m}^{0.486}.$$

*Example 6: an interface crack/corner between two dissimilar anisotropic materials*

To see the piezo effects, two similar cases as example 5 will be reconsidered by letting the anisotropic materials be the ones of PZT-7A and PZT-5H excluding their

piezoelectric constants. By using the same formulae and solution techniques as example 1, the singular orders and stress intensity factors of this problem are calculated as follows.

Interface crack:

$$\delta = 0.5 \pm 0.008i, 0.5,$$

$$K_I = 0.177\text{MPa}\sqrt{\text{m}}, K_{II} = -0.003\text{MPa}\sqrt{\text{m}}, K_{III} = 0,$$

which agree very well with the analytical solutions provided in the literature (Hwu, 1993).

Interface corner:

$$\delta = 0.487,$$

$$K_I = 0.210\text{MPa} \times \text{m}^{0.487}, K_{II} = 0.012\text{MPa} \times \text{m}^{0.487}, K_{III} = 0.$$

Once again, like the crack/corner in homogeneous materials or lying between two dissimilar anisotropic materials, the results of examples 5 and 6 show that both of  $K_I$  and  $K_{II}$  will also increase due to the change from crack to corner when the plates are made by the piezoelectric materials. Whereas the piezoelectric constants influence mostly on the appearance of the electric intensity factor, and have insignificant effect on the magnitude of singular orders and intensity factors of stresses.

## 7 Problem types – 2D or 3D

Although the near tip solutions and the complementary solutions needed for the H-integral (8) are derived based upon the assumptions of two-dimensional deformation, it has been proved (Kuo and Hwu, 2009) that through the modification of H-integral all the solution techniques can be further applied to the associated three-dimensional problems. The reasons for this successful application are: (1) along the 3D crack/corner front each point can be treated as a tip of 2D crack/corner which can be considered to be in generalized plane stress condition for crack/corner in the outer portion and in generalized plane strain condition for crack/corner in the inner portion; (2) besides the typical 2D stress/strain components, the additional third directional stress/strain components such as  $\sigma_{13}$ ,  $\sigma_{23}$  and  $\varepsilon_{13}$ ,  $\varepsilon_{23}$  are all available in the near tip solutions obtained by employing Stroh formalism for two-dimensional anisotropic elasticity (Hwu, et al, 2003; Hwu and Lee, 2004).

Followings are two examples about the edge cracks in isotropic materials. One is under plane strain condition, and the other is under three-dimensional condition. To know the difference induced by the consideration of three-dimensional deformation, same geometry and material properties are used in these two examples.

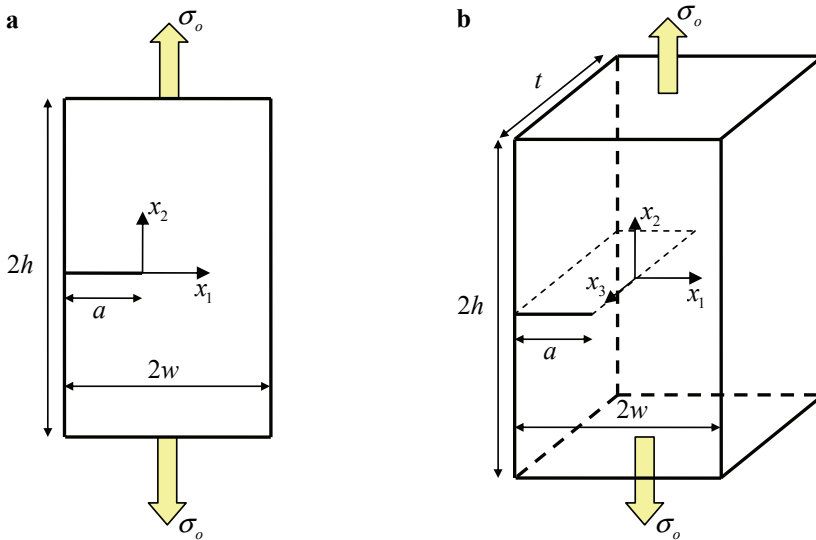


Figure 2: (a) An edge crack in a homogeneous isotropic material (2D); (b) a through thickness edge crack in a homogeneous isotropic material (3D).

*Example 7: an edge crack in a homogeneous isotropic material (2D)*

An edge crack embedded in an isotropic plate under plane strain assumption is discussed in this example. The geometry of this plate is plotted in Figure 2(a) in which  $a = 1\text{mm}$ ,  $a/w = 1$  and  $h/w = 1.75$ . The uniform tension applied at the ends of the plate is  $\sigma_0 = 1\text{MPa}$ . The Young's modulus and Poisson's ratio of this isotropic plate are  $210\text{GPa}$  and  $1/3$ . It is worthy to note that the local environments of the edge crack and center crack are the same and the difference of these two geometries comes from the external environments which will be reflected through the vector  $\mathbf{h}$  containing the values of H-integral. As the statement in example 1, the most critical singular order of stress generated in this example is a triple root  $0.5$  because the crack is within a homogeneous elastic material. Similarly, using eq. (8)<sub>1</sub> and eq. (9) the stress intensity factors can be calculated as

$$K_I = 0.158\text{MPa}\sqrt{\text{m}}, K_{II} = -0.169 \times 10^{-5}\text{MPa}\sqrt{\text{m}}.$$

Normalization of  $K_I$  leads to  $K_I/\sigma_0\sqrt{\pi a} = 2.817$  which is close to the stress intensity factors of the inner part of the through thickness edge crack for the three dimensional case discussed in the next example (see Figure 2(b)).

*Example 8: a through thickness edge crack in a homogeneous isotropic material (3D)*

Consider a rectangular parallelepiped with a through thickness edge crack under remote tension as shown in Figure 2(b) where the parameters  $a$ ,  $t$ ,  $h$ , and  $w$  are the crack length, thickness, half height, and half width of this rectangular solid. The remote tension  $\sigma_o$  is specified as 1MPa, while  $a$  is equal to 1mm. The other dimensions of the specimen are  $a/w = 1$ ,  $h/w = 1.75$ , and  $t/w = 3$ , where  $x_3 = \pm t/2$  are the free surfaces. This rectangular specimen is composed of an isotropic material with Young's modulus  $E = 210\text{GPa}$  and Poisson's ratio  $\nu = 1/3$ . To have the same situation as the comparing published results presented by (Raju and Newmann, 1977; Li, *et al.*, 1998; Sukumar, *et al.*, 2000), when performing the finite element analysis, the boundary conditions are set to be  $u_3 = 0$  on the surface  $x_3 = 0$  due to symmetry, while  $u_1 = u_2 = 0$  on the line  $x_1 = w$  &  $x_2 = 0$ . Figure 3 is a plot of the normalized stress intensity factor  $K_I/\sigma_o\sqrt{\pi a}$  versus the position of crack front  $x_3/t$ . From this plot we see that the present results well agree with the numerical results presented in the literatures (Raju and Newmann, 1977; Li, *et al.*, 1998; Sukumar, *et al.*, 2000) since all the deviations are below 4.03%.

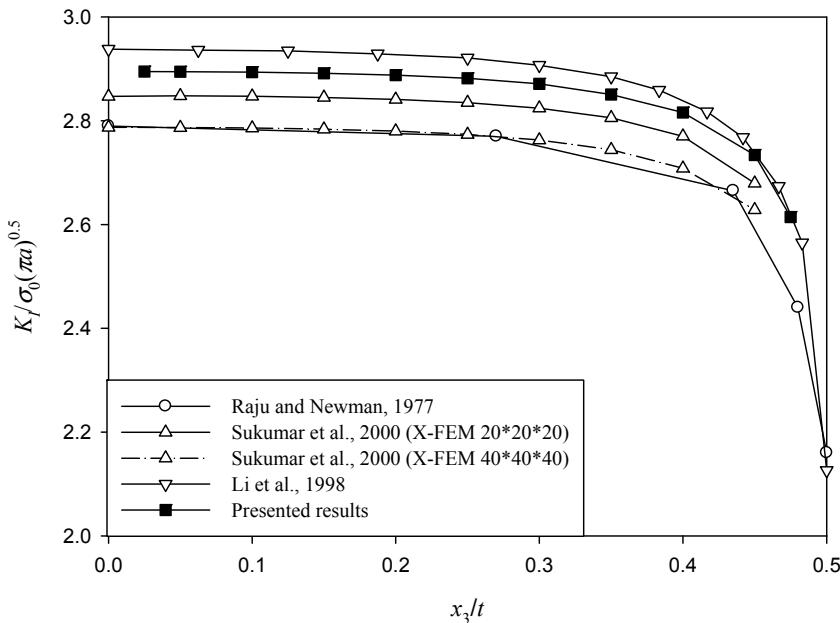


Figure 3: Normalized stress intensity factor  $K_I/\sigma_o\sqrt{\pi a}$  versus the crack front location  $x_3/t$  for a through thickness edge crack in a homogeneous isotropic material subjected to remote tension.

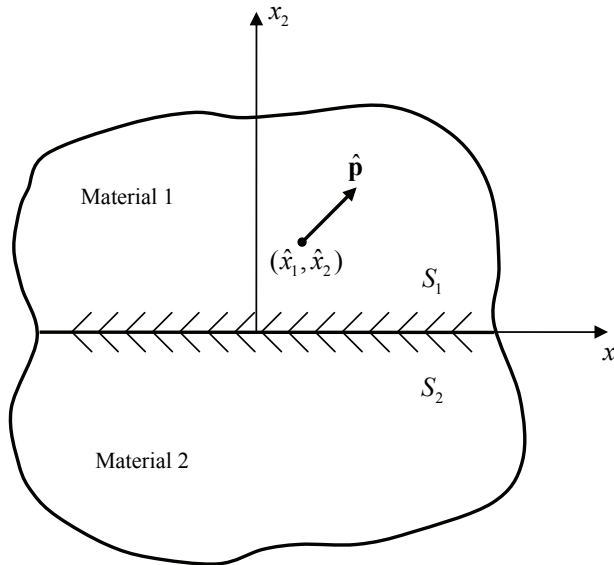


Figure 4: A concentrated force in bimetals.

### 8 Green's functions for interface problems

Consider a bimaterial that consists of two dissimilar anisotropic or piezoelectric elastic half-spaces. Let the upper half-space  $x_2 > 0$  be occupied by material 1 and the lower half-space  $x_2 < 0$  be occupied by material 2 (Figure 4). Assume these two dissimilar materials are perfectly bonded along the interface  $x_2 = 0$ . The Green's function for interface problems is the elasticity solution for a bimaterial subjected to a concentrated force  $\hat{\mathbf{p}}$  applied at point  $\hat{\mathbf{x}} = (\hat{x}_1, \hat{x}_2)$  of material 1. Its solution has been found by using Stroh formalism, that is (Ting, 1996)

$$\begin{aligned} \mathbf{u}_1 &= 2\text{Re}\{\mathbf{A}_1[\mathbf{f}_0(z^{(1)}) + \mathbf{f}_1(z^{(1)})]\}, \quad \boldsymbol{\phi}_1 = 2\text{Re}\{\mathbf{B}_1[\mathbf{f}_0(z^{(1)}) + \mathbf{f}_1(z^{(1)})]\}, \\ \mathbf{u}_2 &= 2\text{Re}\{\mathbf{A}_2\mathbf{f}_2(z^{(2)})\}, \quad \boldsymbol{\phi}_2 = 2\text{Re}\{\mathbf{B}_2\mathbf{f}_2(z^{(2)})\}, \end{aligned} \tag{11}$$

in which  $\text{Re}$  denotes the real part of a complex number;  $(\mathbf{A}_1, \mathbf{B}_1)$  and  $(\mathbf{A}_2, \mathbf{B}_2)$  are

material eigenvector matrices of material 1 and 2; and

$$\begin{aligned} \mathbf{f}_0(z^{(1)}) &= \frac{1}{2\pi i} \langle \ln(z_\alpha^{(1)} - \hat{z}_\alpha^{(1)}) \rangle \mathbf{A}_1^T \hat{\mathbf{p}}, \\ \mathbf{f}_1(z^{(1)}) &= \frac{1}{2\pi i} \sum_{j=1}^3 \langle \ln(z_\alpha^{(1)} - \bar{\hat{z}}_j^{(1)}) \rangle \mathbf{A}_1^{-1} (\bar{\mathbf{M}}_2 + \mathbf{M}_1)^{-1} (\bar{\mathbf{M}}_2 - \bar{\mathbf{M}}_1) \bar{\mathbf{A}}_1 \mathbf{I}_j \bar{\mathbf{A}}_1^T \hat{\mathbf{p}}, \quad (12) \\ \mathbf{f}_2(z^{(2)}) &= -\frac{1}{2\pi} \sum_{j=1}^3 \langle \ln(z_\alpha^{(2)} - \hat{z}_j^{(1)}) \rangle \mathbf{A}_2^{-1} (\mathbf{M}_2 + \bar{\mathbf{M}}_1)^{-1} \mathbf{A}_1^{-T} \mathbf{I}_j \mathbf{A}_1^T \hat{\mathbf{p}}, \end{aligned}$$

where

$$\begin{aligned} z_\alpha^{(k)} &= x_1 + \mu_\alpha^{(k)} x_2, \quad \hat{z}_\alpha^{(k)} = \hat{x}_1 + \mu_\alpha^{(k)} \hat{x}_2, \quad k = 1, 2, \\ \alpha &= 1, 2, 3 \text{ (anisotropic), } \alpha = 1, 2, 3, 4 \text{ (piezoelectric)}. \end{aligned} \quad (13)$$

The overbar denotes the complex conjugate;  $\mathbf{I}_j$  is a diagonal matrix with unit value at the  $jj$  component and all the others are zero;  $\mu_\alpha^{(1)}$  and  $\mu_\alpha^{(2)}$  are material eigenvalues of material 1 and 2; and  $\mathbf{M}_1$  and  $\mathbf{M}_2$  are the *impedance matrices* defined by

$$\mathbf{M}_1 = -i\mathbf{B}_1\mathbf{A}_1^{-1}, \quad \mathbf{M}_2 = -i\mathbf{B}_2\mathbf{A}_2^{-1}. \quad (14)$$

## 9 A special boundary element for interface problems

Based upon the Green's functions shown in (10), a special boundary element for interface problems can be designed by following the standard procedure of boundary element formulation (Brebbia, *et al.*, 1984). To show the improvement of this special boundary element, one typical example about the interface corners is presented in this section.

*Example 9: an edge interface corner between two dissimilar materials*

Since the development of this special boundary element is for the improvement of the computational accuracy and efficiency of interface problems, the example considered here is an interface edge corner (Figure 5) treated in our previous study (Hwu and Kuo, 2007). The material above the interface is isotropic whose properties are:  $E = 10$  GPa and  $\nu = 0.2$ , and the material below the interface is orthotropic whose properties are the same as those given in Example 1. The reference length used in the definition (7) is selected to be  $b = 5$  mm.

The difference between the present example and our previous study comes from the source of the displacement and traction vectors  $\mathbf{u}$  and  $\mathbf{t}$  of the actual system needed in the calculation of H-integral (8). In our previous study  $\mathbf{u}$  and  $\mathbf{t}$  are calculated by the commercial finite element code ANSYS, while in the present example

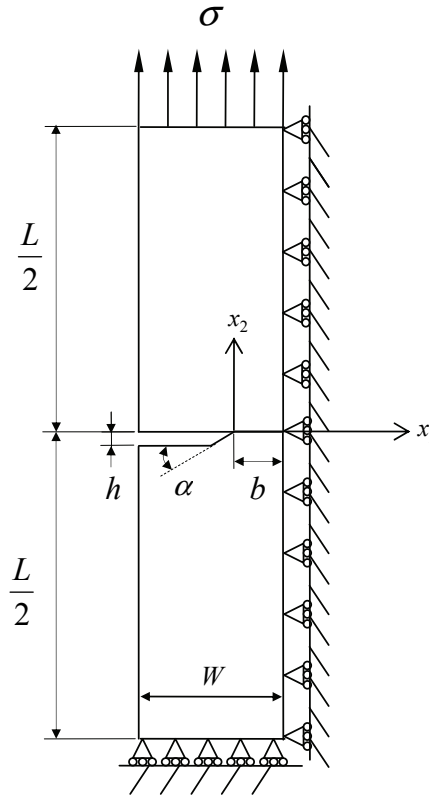


Figure 5: An edge interface corner between two dissimilar materials. ( $b = 5\text{mm}$ ,  $b/W = 1/3$ ,  $h/W = 1/15$ ,  $b/L = 1/18$ ,  $\alpha = 30^\circ$ ,  $\sigma = 10\text{GPa}$ )

they are calculated by the special boundary element introduced in this paper. In ANSYS, PLANE42 element is selected for the present problem. Table 2 shows the stresses at the interfacial point  $(2,0)$  versus the element number, from which we see that the stresses above and below the interface calculated from ANSYS are discontinuous, which is incorrect and will approach to the same values only when very fine meshes are used near the interfaces. On the other hand, the solutions obtained from the special boundary element will always provide continuous stresses across the interface. Figure 6 shows the variation of the stresses along the interface  $(0 \leq x_1 \leq 5, x_2 = 0)$  by using 22614 elements for ANSYS and 279 elements (no element meshes are needed along the interface) for present BEM, from which we see that the stresses have the tendency to approach infinity near the corner tip and the stress discontinuity through ANSYS modeling becomes much more inevitable.

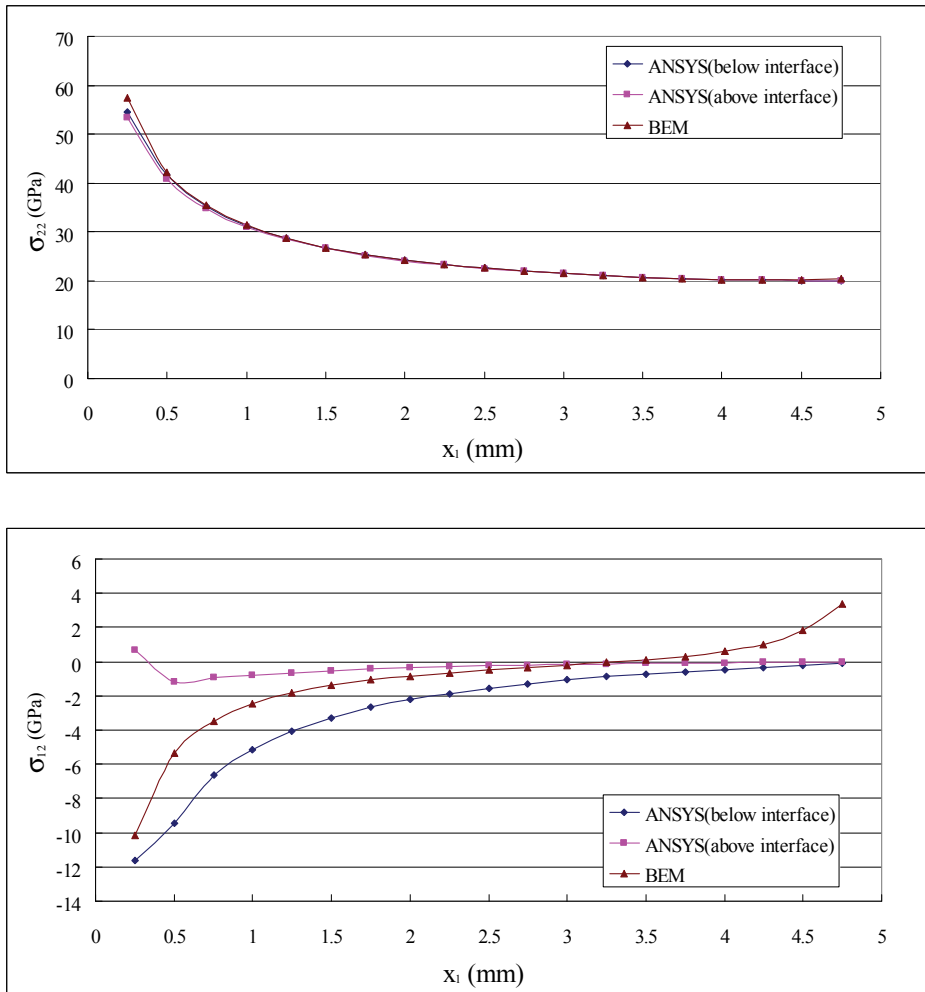


Figure 6: The stresses along the interface calculated by ANSYS and present BEM. (ANSYS: 22614 elements; BEM: 279 elements)

Due to this difference we believe the present results shown in Table 3 is more accurate than the one shown in (Hwu and Kuo, 2007). Note that in Table 3,  $r$  stands for the radius of the circular path originated at the corner tip for the H-integral. In addition to the theoretical proof provided in (Hwu and Kuo, 2007), the path independent property of H-integral can also be confirmed through this numerical computation in which several different paths are used.

Table 2: Interfacial stresses at point (2,0) versus element number.

$\sigma_{yy}$ (GPa)				
ANSYS				
element number	1361	5552	22614	75127
above interface: $\sigma_{yy}^+$	22.929	23.775	24.113	24.290
below interface: $\sigma_{yy}^-$	23.582	23.949	24.197	24.329
difference: $\sigma_{yy}^+ - \sigma_{yy}^-$	-0.653	-0.174	-0.084	-0.039
average: $(\sigma_{yy}^+ + \sigma_{yy}^-)/2$	23.256	23.862	24.155	24.310
present BEM				
element number	76	101	129	279
$\sigma_{yy}$	23.710	23.780	24.210	24.210
$\sigma_{xy}$ (GPa)				
ANSYS				
element number	1361	5552	22614	75127
above interface: $\sigma_{xy}^+$	0.659	0.160	-0.356	-0.6797
below interface: $\sigma_{xy}^-$	-2.734	-2.488	-2.220	-1.729
difference: $\sigma_{xy}^+ - \sigma_{xy}^-$	3.392	2.6483	1.865	1.049
average: $(\sigma_{xy}^+ + \sigma_{xy}^-)/2$	-1.037	-1.164	-1.288	-1.204
present BEM				
element number	76	101	129	279
$\sigma_{xy}$	-0.648	-0.668	-0.834	-0.836

Table 3: Comparison of the stress intensity factors calculated with the data provided by ANSYS and present BEM.

$r$ (mm)	$K_I(\text{MPa} \times \text{mm}^{0.467})$	$K_{II}(\text{MPa} \times \text{mm}^{0.467})$
Present (with BEM)		
$r = 0.5$	70.990	9.541
$r = 0.6$	71.053	9.612
$r = 0.7$	71.069	9.656
$r = 0.8$	71.116	9.673
Hwu and Kuo (2007)		
$r = 0.5625$	72.772	9.154
$r = 0.6750$	72.859	9.260
$r = 0.7875$	72.935	9.347

### 10 Concluding remarks

In this paper several different kinds of interface problems are solved by using the same formulae and solution techniques. Through the same definition, the stress

intensity factors of interface corners and cracks which are usually defined independently can now be discussed and compared under the same situation set by the users. By numerical examples shown in this paper, the combination of special boundary element and the path-independent H-integral is also proved to be a good approach dealing with the interface problem.

**Acknowledgement:** The authors would like to thank the National Science Council, TAIWAN, R.O.C. for support through Grant NSC 95-2221-E-006-144-MY3.

## References

- Attaporn, J. A.; Koguchi, H.** (2009): Intensity of stress singularity at a vertex and along the free edges of the interface in 3D-dissimilar material joints using 3D-enriched FEM. *CMES: Computer Modeling in Engineering and Sciences*, vol. 39, pp. 237-262.
- Brebbia, C.A.; Telles, J.C.F.; Wrobel, L.C.** (1984): Boundary element techniques: theory and applications in engineering, Springer-Verlag, NY.
- Hwu, C.** (1993): Explicit solutions for the collinear interface crack problem. *Int J Solids Struct*, vol. 30 (3), pp. 301-312.
- Hwu, C.; Omiya, M.; Kishimoto, K.** (2003): A key matrix N for the stress singularity of the anisotropic elastic composite wedges. *JSME Int J Series A*, vol. 46 (1), pp. 40-50.
- Hwu, C.; Lee, W. J.** (2004): Thermal effect on the singular behaviour of multi-bonded anisotropic wedges. *J Therm Stresses*, vol. 27 (2), pp. 111-136.
- Hwu, C.; Kuo, T. L.** (2007): A unified definition for stress intensity factors of interface corners and cracks. *Int J Solids Struct*, vol. 44, pp. 6340-6359.
- Hwu, C.; Ikeda, T.** (2008): Electromechanical fracture analysis for corners and cracks in piezoelectric materials. *Int J Solids Struct*, vol. 45, pp.5744-5764.
- Kuo, T. L.; Hwu, C.** (2009): Multi-order stress intensity factors along three-dimensional interface corners. *J Appl Mech, Trans ASME*, in press.
- Labossiere, P. E. W.; Dunn, M. L.** (1999): Stress intensities at interface corners in anisotropic bimetals. *Engrg Fract Mech*, vol. 62, pp.555-575.
- Li, S.; Mear, M. E.; Xiao, L.** (1998): Symmetric weak-form integral equation method for three-dimensional fracture analysis. *Comput Methods Appl Mech Engrg*, vol. 151, pp. 435-459.
- Liu, K.Y.; Long, S.Y.; Li, G.Y.**(2007) A Meshless Local Petrov-Galerkin Method for the Analysis of Cracks in the Isotropic Functionally Graded Material *CMC: Computers, Materials & Continua*, Vol. 7, No. 1, pp. 43-58.

**Ou, Z. C.; Wu, X.** (2003): On the crack-tip stress singularity of interfacial cracks in transversely isotropic bimetals. *Int J Solids Struct*, vol. 40, pp. 7499-7511.

**Raju, I. S.; Newmann Jr, J. C.** (1977): Three-dimensional finite element analysis of finite-thickness fracture specimens. Technical Report TND-8414, NASA, USA.

**Sanz, J. A.; Solis, M.; Dominguez, J.** (2007): Hypersingular BEM for piezoelectric solids: formulation and applications for fracture mechanics. *CMES: Computer Modeling in Engineering and Sciences*, vol. 17, pp. 215-229.

**Shah, P.D.; Tan, C.L.; Wang, X.** (2006): Evaluation of T-stress for an interface crack between dissimilar anisotropic materials using the boundary element method. *CMES: Computer Modeling in Engineering and Sciences*, vol. 13, pp. 185-197.

**Sukumar, N.; Moes, N.; Moran, B.; Belytschko, T.** (2000): Extended finite element method for three-dimensional crack modelling. *Int J Numer Methods Engrg*, vol. 48, pp. 1549-1570.

**Ting, T. C. T.** (1996): *Anisotropic Elasticity: Theory and Applications*, Oxford Science Publications, NY.

**Vodicka, R.; Mantic, V.; Paris, F** (2007): Extended Symmetric Variational Formulation of BIE for Domain Decomposition Problems in Elasticity – An SGBEM Approach for Nonconforming Discretizations of Curved Interfaces. *CMES: Computer Modeling in Engineering and Sciences*, vol. 17, no. 3, pp. 173-204.

